IOSR Journal Of Pharmacy And Biological Sciences (IOSR-JPBS)
e-ISSN:2278-3008, p-ISSN:2319-7676. Volume 14, Issue 4 Ser. I (Jul–Aug 2019), PP 57-65
www.Iosrjournals.Org

Optimization of Chitosan Nanoparticles for Direct Nose-To Brain Sumatriptan Deposition

Hend Mohamed Abdel-Bar
Department of Pharmaceutics and Industrial Pharmacy, Faculty of Pharmacy, University of Sadat City, Egypt
Corresponding Author:Hend Mohamed Abdel-Bar

Abstract:*The aim of this study was to optimize different chitosan nanoparticles to improve sumatriptan brain uptake. Different chitosan nanoparticles (CS NPs) were prepared by cross linking CS with tripolyphosphate (TPP). The NPs were statistically optimized by Box-Behnken design using Design Expert® software (Version 9.0.6.2, Stat-Ease Inc. Minneapolis, MN, USA). The influence of CS and TPP concentrations as well as stirring speed on particle size and entrapment efficiency (EE%) were evaluated. The optimized formulae were evaluated concerning zeta potential, TEM and in vitro release. Plasma pharmacokinetics and brain deposition were also investigated following intranasal administration and compared to the intravenous route. Increasing chitosan and/ or decreasing the stirring speed increased the particle size. Moreover, EE% was positively affected by polymer concentration and inversely proportional to stirring speed. The optimized positively charged formulae were non-aggregated spherical in shape with a particle size of 73.5±1.25nm and EE% of 71.69±3.24%. The selected CS NPs improved sumatriptan brain uptake by 2.38 fold more than intravenoussumatriptan solution. The achieved results elected intranasal sumatriptan CS NPsas a possible strategy to traverse the blood-brain barrier.*

Keywords:*Brain uptake, Chitosan, Intranasal, Nanoparticles, Sumatriptan*

Date of Submission: 10-07-2019 Date of acceptance: 25-07-2019

I. Introduction

Migraine is a worldwide disorder that devastating pain that negatively affects patients' quality of life[1].Among different antimigraine drugs, sumatriptan is widely used in the treatment of acute migraine through its vasoconstrictor effect on the meningealvessels that averts the transmission of nociceptive in the brain [2]. Unfortunately, sumatriptan exerts incomplete drug absorption as well as pre-systemic metabolism with low oral bioavailability of 15% only [3]. Moreover, the blood-brain barrier (BBB) is a complex barrier that reserves the brain by its selective permeability to the essential molecules only. Thus the BBB hinders the drug uptake to the brain via the systemic circulation [4].

Different studies proved the ability of polymericnanoparticles to cross the BBB and deliver their payload to the brain [4]. The small sizes with high surface area increase the contact area of the NPs with the epithelial surface and in turn allow a greater cellular internalization through both transcytosis and endocytosis [5].Among different polymers, CS is broadly employed as a drug carrier as it is a non-toxic, biocompatible, biodegradable and mucoadhesive polymer [6]**.**The mucoadhesion action of CS was owing to its cationic charge that allows electrostatic attraction with the negatively charged mucus [7].Previous literature proved the ability of CS NPs to improve the brain uptake [8, 9]. Regarding the brain delivery, intranasal (IN) delivery has different advantages over the systemic administration via the intravenous (IV) route. IN route allow the direct drug transport with high percentage via the olfactory bulb thus decrease the systemic distribution of the drugs that minimize the associated systemic adverse effects [10].

Therefore, the aim of the present study was to prepare and optimize different sumatriptan loaded CS NPs for possible brain targeting via the intranasal cavity. Different CS NPs were prepared by ionic gelation method and optimized to obtain NPs with minimum particle size and maximum entrapment efficiency (%). The plasma pharmacokinetics and brain distribution studies were also conducted to elucidate the ability of the proposed system to improve sumatriptan brain delivery.

II. Materials and Method

1. Materials

Low molecular weight chitosan (CS) (MW50000-190000D, degree of deacetylation ≈90%), sumatriptan succinate, acetonitrile, triethylamine, HEPES, MTT, dimethyl sulfoxide (DMSO) and fetal bovine serum (FBS) were obtained from Sigma, USA. Tripolyphosphate (TPP) was supplied from BDH Chemicals, England. Tween 80, glacial acetic acid, potassium dihydrogen orthophosphate, sodium hydroxide, sodium

chloride, potassium chloride, sodium dibasic hydrogen orthophosphate, hydrochloric acid and Tween 80 (polysorbate 80): obtained from FlukaChemika-BioChemika, Switzerland.Gentamycin and minimum essential medium were purchased from Gibco, Invitrogen, UK.

2. Method

2.1. Experimental design

In this study, the influence of three variables each at three levels was inspected using Box-Behnken design (BBD) to optimize sumatriptan loaded CS nanoparticles (NPs). Design-Expert software (Design-Expert 9.0.5.2, State-Ease Inc., USA) was used to construct BBD and explore both the response surfaces and the statistical models [11]**.** The selected critical process parameters (CPPs) or the independent variables were CS concentration, TPP concentration and stirring speed. The particle size (*Y1*) and entrapment efficiency (EE %) (*Y2*) were selected as the critical quality attributes (CQAs). The influence of different fabrication variables on sumatriptan CS NPs was investigated to obtain NPs with the following quality target product profile (QTPP); minimum particle size and maximum EE% **(Table 1)**. All the responses observed were simultaneously fittedto linear; two-factor interactions (2FI) and quadratic models. Various statistical indices such as P-values,F values, R^2 squared values (adjusted R^2 and predicted R^2) and predicted residual error sum of squares (PRESS) were used to assess the statistical significance of the models. Various 3-D response surface plots were constructed by the software and the polynomial equations were authenticated. Different feasibilities were conductedover the experimental domain to find the compositionsof the optimized NPs. All experiments were performed in triplicate to validate the final predicted results compared to the experiments.

Based on the highest desirability, the design space was created to define the optimum CPPs to prepare NPs with the desired QTPP [12]. Hence, one optimum checkpoint was picked to validate the chosen experimental domainand the polynomial equations. The experimental values of theresponses were quantitatively compared with that of the predictedvalues and prediction error (%) were calculated.The linear regression plots between observed and predictedvalues of the responses were obtained.

2.2. Preparation of sumatriptanchitosan nanoparticles

Briefly, CS solutions (pH 5.5) with different concentrations were prepared by dissolving the polymer in an aqueous solution of glacial acetic acid (1%v/v) under magnetic. Subsequently, Tween 80 (1%w/v) and sumatriptan (10% w/v) wereadded to the polymer solutions. TPP aqueous solutions (pH 3)were prepared with different concentrations as reported in **Table(1)**. TPP solutions were added dropwise to CS solutions in a ratio of 1:3 v/vunder continuous stirring for 60 min [13]. Consequently, the resultant NPs dispersions were centrifuged at 15000rpm for 30 min at 4°C. The obtained pellets were re-dispersed into PBS (pH 7.4) and stored at 4 °C for further analysis.

Table 1: Critical process parameters with their levels, critical quality attributes and quality target product profile

Critical process parameters (Coded independent variables)	Levels		
	Low (-1)	Medium (0)	High (+1)
A: CS concentration (% w/v)	0.05	0.225	0.4
B: TPP concentration (% w/v)	0.05	0.225	0.4
C: Stirring speed (rpm)	500	750	1000
Critical Quality attributes (Responses)	Quality target product profile (constrains)		
Y1: Particle size (nm)	Minimize		
Y2: Entrapment efficiency (%)	Maximize		

2.3. *Invitro* characterization of the prepared sumatriptan loaded chitosan nanoparticles

2.3.1. Particle size, size distribution and zeta potential

The particle size (z-average) and size distribution expressed as polydispersity index (PDI) of the prepared NPs as well as zeta potential of the optimized NPs dispersed in deionized water were estimated by dynamic light scattering technique at 25ºC using an angle of 90° [14]**.**

2.3.2. Entrapment efficiency (EE %)

The entrapment efficiency (EE%) was determined indirectly where 5mL of the prepared sumatriptan CS NPs was centrifuged at 12000 rpm for 30min at 4°C. The amount of sumatriptan in the supernatant was quantified using HPLC method[3]. Briefly, a reverse phase C_{18} column (Thermo® BDS, 250X4.6 mm, 5µm) was used at 25°C. The mobile phase consisted of 0.05 M potassium dihydrogen phosphate containing 0.1% v/v triethylamine(pH 3.8) and acetonitrile (80:20 v/v). The flow rate was adjusted to 1 mL/ min and samples were detected at 226 nm.

The EE was calculated according to the following equation and the appropriate entrapment efficiency was reported as a percent.

$$\mathbf{EE\%}=\frac{\mathbf{Totalamountofsumatriptanadded-amountoffreesumatriptaninthesuprnatant}}{\mathbf{Totalamountofsumatriptanadded}}\times\mathbf{100}$$ Eq. (1)

2.3.3. Transmission electron microscope (TEM)

The optimized sumatriptan CS NPs were visualized using TEM. A drop of the NPs was deposited on a copper 300-mesh grid, coated with carbon and was allowed to stand for 10min after which, any excess fluid was absorbed by a filter paper. Before the examination, one drop of 1% phosphotungstic acid was applied and allowed to dry for 5min.

2.3.4. *In vitro*sumatriptan release study

The*in vitro*sumatriptan release study from the optimized CS NPs was executed using dialysis membrane methodin simulated nasal fluids (100 mL, pH 7.4) for 8h [15]. An aliquot volume of the prepared NPs (equivalent to 10mg sumatriptan) was placed in the pre-soaked dialysis membrane (cut off: 10,000-12,000D). The dialysis bag was attached to the USP apparatus shaft and stirred at 100rpm ±0.1 at 37±0.5°C. At predetermined time intervals, an aliquot of 1mL of the dissolution medium was withdrawn and replaced by the same volume of the medium. The amount of sumatriptan released was quantified using the previously mentioned validated HPLC method.

2.4. Nasal integrity study

The *in vitro* cytotoxicity of the optimized sumatriptan CS NPs was performed on Calu- 3 cells using MTT assay technique. The cells were grown in minimum essential medium containing 10% heat-inactivated FBS, 1% L-glutamine, 50 mg/mL gentamicin and HEPES buffer at 37°C under a humidified atmosphere containing 5% CO_2 (Thermo Scientific Forma®, Germany). The cells were seeded in 96-well plate with a seeding density of 10K/well. Subsequently, the cells were treated with a serial concentration of the prepared sumatriptanCS NPs in range of 0.01-100 µM at 37°C for 24 h. Afterward, the cells were incubated with 120 µL of MTT solution (5 mg/mL, pH 7.4) at 37°C for 4 h. The formed complex was dissolved in dimethyl sulfoxide and the absorbance was detected spectrophotometrically at 570 nm by plate reader (ChroMate-4300, FL, USA). The cell viability was assessed in corresponding to the cell viability of the untreated control cells [16]**.**

2.5. *In vivo* pharmacokinetics and biodistribution studies

All the *in vivo* studies were approved by the Ethics Committee at the faculty of Pharmacy, University of Sadat City, Egypt.

2.5.1. Animal handling and drug dosing

Ninety-six male albino rats weighing 200 g±10% were equally divided into 2 groups (48 rats in each group). Rats were retained in plastic cages at 25°C with 12 h light/dark cycle. They were nourished on rodent chow with free access for water. Prior to the experiment, animals were anesthetized by intramuscular injection of 50 mg/ kg ketamine. Sumatriptan was administrated in a single dose of 5 mg/Kg. The animals in group 1received 10 µL of the optimized intranasal sumatriptan CS NPs in each nostril. The intranasal administration was performed by the aid of high-performance micropipette (Robfield-GmbttKobenicker, Strabe 320 Deutsch Land) with 0.1 mm in diameter tip. While animals in group 2 received intravenous bolus injection of sumatriptan solution via the tail vein. Blood samples were collected by cardiac puncture at the following time intervals; 5, 10, 15, 30, 60, 120, 240 and 480 min in EDTA containing test tubes. Blood samples were centrifuged at 9000 rpm for 15 min and the obtained plasma were separated. Consequently, animals were subjected to brain segmentation. The collected brains were homogenized in distilled water at 25000 rpm using tissue homogenizer. All plasma and brain samples were kept at -80°C for further analysis. The concentration of sumatriptan and brain homogenate were quantified by the previously mentioned HPLC method [3]**.**

2.5.2. Pharmacokinetics calculations:

Different pharmacokinetic parameters were calculated using Wagner-Nelson Method. The absolute bioavailability (F %) of the optimized intranasal sumatriptan CS NPs was calculated according to the following equation [17]:

$$F\ \% = \frac{\text{AUC 0–t (intranasal)}}{\text{AUC 0–t (intravenous)}} * 100$$ Eq. (2)

The drug targeting efficiency (DTE %) to the brain and direct nose to brain transport (DTP %) were determined using the following equations [17]:

$$DTE\ \% = \frac{\text{AUC brain /AUC plasma (intranasal)}}{\text{AUC brain /AUC plasma (intravenous)}} * 100 \quad \text{Eq. (3)}$$

$$DTP\ \% = \frac{Bintr\ anasal\ - Bx}{Bintranasal} * 100 \quad \text{Eq. (4)}$$

Where $Bx = \frac{Bintravenous}{Pintravenous} * Pintranasal$

Where: Bx is the brain $AUC_{0–480}$ following intranasal administration, B intravenous is the $AUC_{0–480}$ in the brain following intravenous administration, P intravenous is the $AUC_{0–480}$ in plasma post intravenous administration. While, B intranasal is the $AUC_{0–480}$ in the brain following intranasal administration, P intranasal is the $AUC_{0–480}$ in plasma after intranasal administration.

3. Statistical analysis

All the *in vitro* data are expressed as the mean of three replicates ± SD while six replicates for the *in vivo* results ± SE. Student-t test was used to compare between two variables while one-way analysis of variance (ANOVA) followed by Tukey HSD test was applied to compare between groups, using SPSS 18 (Chicago, U.S.A.). The differences were statistically significant at a probability level (p) less than 0.05.

III. Results and discussion

The ionic gelation technique was selected to prepare CS NPs where the dropwise addition of TPP aqueous solution to CS solution resulted in the formation of nanoparticles. NPs were spontaneously fabricated due to the electrostatic interaction between the CS chains and TPP as a cross-linker [18]. The appearance of opalescence dispersion revealed the formation of nanoparticles, which was thought to be the result of the electrostatic interaction between the positively charged amino groups of CS polymer and the negatively charged TPP [19]**.**

Previous literature reported that the intranasal delivery of nanocarriers with particle size less than 100 nm were suggested to be taken via the intraaxonal route because their diameter was less than that of the axons in the filiaolfactoria [17]. Therefore, the process parameters were optimized to have sumatriptan CS NPs with minimum particle size (less than 100 nm) and maximum EE %. Therefore, the adopted BBD had 17 runs to investigate the effect of different process parameters on CS NPs size and EE % **(table 2)**. According to the highest R^2 and the lowest PRESS values, the quadratic model was selected as the best fit statistical model describing the influence of different CPPs on particle size and EE% as CQAs**(table 3)**.

Table (2): Experimental design matrix including critical process parameters with related critical quality attributes

Run	CS concentration (% w/v)	TPP concentration (% w/v)	Stirring speed (rpm)	Particle size (nm)	EE (%)
1	0.225	0.225	750	148±2.54	58±4.78
2	0.05	0.4	750	50±1.24	45±2.21
3	0.225	0.225	750	140±2.41	56±5.14
4	0.225	0.4	1000	120±2.34	50±3.69
5	0.225	0.225	750	138±1.87	56.84±6.14
6	0.4	0.225	500	149±1.56	73.45±2.14
7	0.225	0.05	500	154±3.58	65±3.45
8	0.4	0.4	750	139±5.14	60.5±5.14
9	0.225	0.225	750	140±2.97	59.84±2.12
10	0.225	0.225	750	143±5.21	58.74±1.74
11	0.05	0.05	750	124±1.26	45±1.22
12	0.05	0.225	500	147±3.78	68±1.87
13	0.225	0.05	1000	130±2.54	58±6.14
14	0.4	0.225	1000	135±4.78	70±2.34
15	0.05	0.225	1000	117±3.41	42±5.14
16	0.4	0.05	750	55±5.12	60±2.25
17	0.225	0.4	500	150±2.87	75±3.87

Table (3): Model summary statistics for particle size (Y1) and entrapment efficiency (Y2)

Response	Model	Adequate precision	R^2	Adjusted R^2	Predicted R^2	SD	% CV	p-value
Particle size (nm)	Quadratic	29.97	0.9902	0.9775	0.9020	4.56	3.55	<0.0001
EE (%)	Quadratic	33.15	0.9923	0.9825	0.9668	1.28	2.17	<0.0001

1. The influence of process parameters on sumatriptan chitosan nanoparticles particle size

Table (2) shows that the fabricated sumatriptan CS NPs had a particle size range from 50-154 nm with polydispersity index (PDI) less than 0.4. The effect of various significant CPPs on particle size could be described according to the following equation:

***Particle size* = +141.80+5.00A-12.25C+39.50AB-1.50BC-25.65A^2-24.15B^2+20.85C^2Equation (5).**

By inspecting **equation (5)**, it could be concluded that NPs particle size was directly proportional to ***CS concentration (A)***. The predominant influence of polymer concentration on NPs size could be attributed to the concomitant increase in viscosity observed with high CS concentration. Increasing polymeric solution viscosity could hinder the electrostatic interaction between the positively charged CS amino groups and TPP [20]. Furthermore, at high CS concentration, the energy between polymer chains reduced. Subsequently, a small number of CS molecules would be accessible for cross-linking [21]. Therefore, as the polymer concentration increases the CS molecules would convene together into large particles. The interaction between CS and TPP concentration could be clarified in the 3-D response surface **(Figure 1A)**. The positive regression coefficient sign indicated the predominant effect of CS concentration (A) over TPP concentration (B) on particle size.

The negative influence of ***stirring speed (C)*** on particle size could be due to the mechanical shear that is generated from increasing stirring speed could disrupt the polymer chains and subsequently decrease the particle size [22]**.** As expected, the concomitant increase in TPP and stirring speed had a negative influence on particle size as shown in the 3-D response surface **(Figure 1B)**.

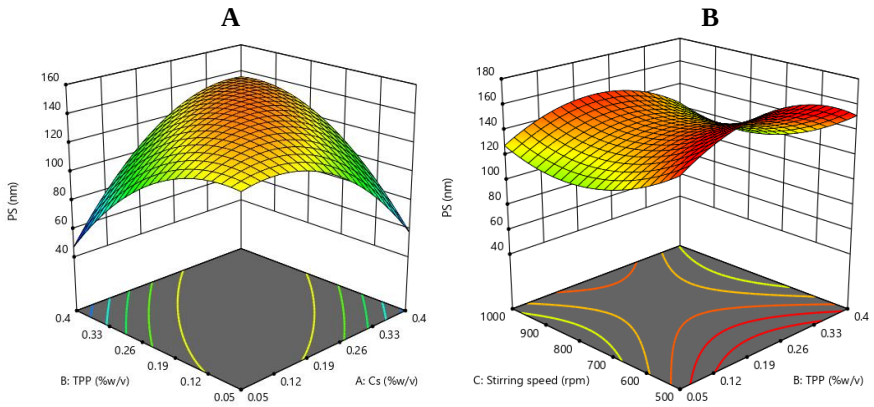

Figure 1: Response 3D plot for the interaction of (A) CS concentration and TPP concentration, (B) TPP concentration and stirring speed on particle size (Y1).

2. Effect of different critical process parameters on entrapment efficiency (Y2).

The sumatriptan EE % ranged from 42-75% in the obtained CS NPs as shown in **Table (2).** The influence of different significant CPPs on EE% could be depicted from the following equation:

EE %= +57.88+7.99A-7.68C+0.125AB-4.50BC-1.95A^2 -3.31B^2 +7.43C^2Equation (6)

By scrutinizing **equation (6)**, a positive correlation between ***CS concentration(A)*** and % EE could be depicted as at high polymer concentration, more domains were available for sumatriptanencapsulation[23]**.** The positive interaction between the CS concentration (A) and TPP concentration (B) could be elucidated from the 3-D response surface **Figure (2A)**. As expected, increasing CS and TPP was accompanied with strengthened electrostatic interaction and consequently the preparation of NPs available for sumatriptan entrapment [24]**.** On the contrary,the entrapment efficiency of sumatriptan is significantly decreased by increase ***stirring speed (C)***.This might be attributed to the leakage of the entrapped sumatriptan from NPs at the high stirring speed [25]. Moreover, the negative coefficient of BC indicated the pronounced negative effect of stirring speed on EE% **(Figure 2B)**.

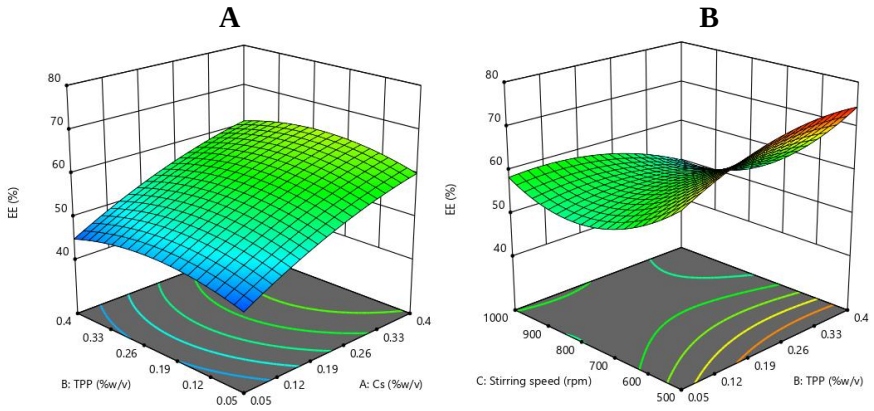

Figure 2: Response 3D plot of (A) the interaction of CS concentration and TPP concentration (B) the interaction of TPP concentration and stirring speed on sumatriptan entrapment efficiency (Y1).

3. Optimization of sumatriptan chitosan nanoparticles

Based on the high desirability, one formulawas selected and prepared as a checkpoint to validate the developed models. **Tables (4)** illustrate the composition, predicted and experimental particle size (Y1) and EE % (Y2), respectively. The linear correlation plots between experimental and predicted values for both responses had high R^2 values (0.9931 and 0.9901 for particle size and EE% respectively). Therefore, the developed models were suitable for studying and predicting the most suitable CPPs for the preparation of sumatriptan CS NPs with the following QTPP; minimum particle size and maximum EE %. Thus this formula was subjected for further studies.Moreover, zeta potential values of the optimized sumatriptan CS NPs was +35.54± 3.12 indicated its stability.

Table 4: The experimental and predicted entrapment efficiency of the optimized sumatriptan chitosan nanoparticles

Response	CS concentration (%w/v)	TPP concentration (%w/v)	Stirring speed (rpm)	Exp.	Pre.	% Pre. error
Particle size (nm)	0.4	0.05	1000	73.5±1.25	72.097	1.91
EE (%)				71.69±3.24	70.063	2.26

4. Transmission electron microscope

TEM reveals that the optimized sumatriptan CS NPs had an almost spherical appearance **(Figure 3).** The diameters of the optimized NPs observed by TEM were in good agreement with the particle size determined by dynamic light scattering technique described above.

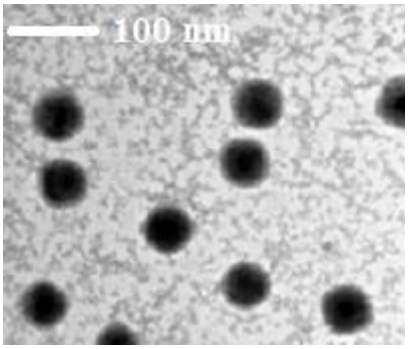

Figure 3: Transmission electron microphotograph of the optimized sumatriptan chitosan nanoparticles.

5. *In vitro*sumatriptan release

The percentage of sumatriptanrelease pattern over timeis depicted in**Figure (4)**.After 8h, the respective percentage sumatriptan released was 95.68 ±3.58. At pH 7.4, CS amino groups with pKa 6.3 are deprotonated, thus forming an insoluble CS matrix thus controlling the drug release over 8 h [26]. Concerning the kinetics of sumatriptan release from the optimized formula, CS NPs showed a zero-order release pattern with R^2 of 0.984.

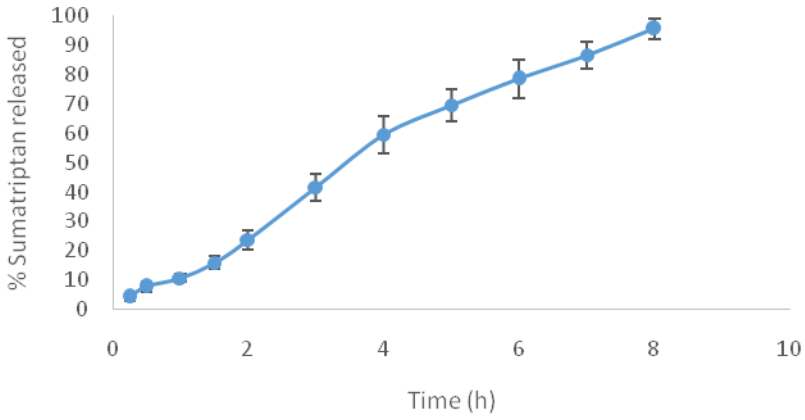

Figure 4:*In vitro* release profile of sumatriptan from chitosan nanoparticle in simulated nasal fluids (pH 7.4) at 37^{o}C.Results are the mean of three replicates ±SD.

6. Nasal integrity study

Nasal cytotoxicity of the optimized sumatriptan CS NPs assessed by MTT assay on Calu3 cells (figure 5). Higher cell viability (> 80%) could be observed after 24 h incubation of different sumatriptan CS NPs up to 10 µM. At higher concentration (100 µM), a slight insignificant decrease in cell viability could be observed (p>0.05). These findings reveal that sumatriptan CS NPs could be considered cytocompatible with good cellular tolerability [16].

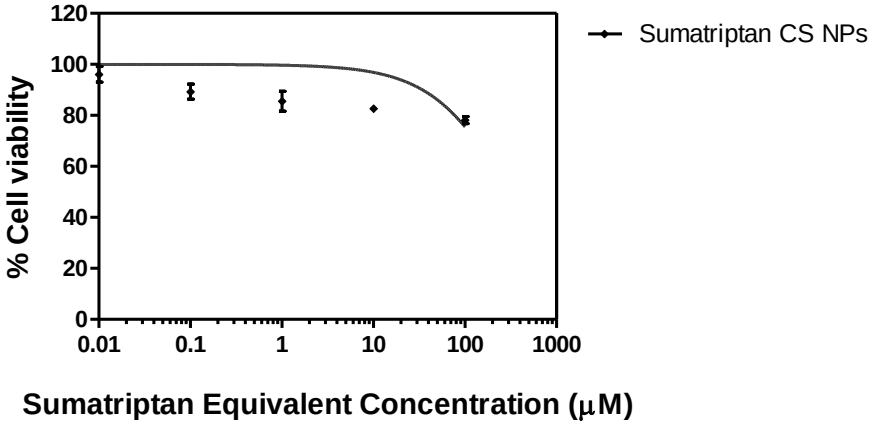

Figure 5:*In vitro* % Calu- 3 Cell viability after 24 hours of exposure to different concentrations of sumatriptan chitosan nanoparticles at 37ºC. Results are the mean of three replicates ±SD.

7. Pharmacokinetic studies and brain biodistribution

The mean plasma and brain sumatriptan concentration-time profiles are illustrated in figure 6A and B. The calculated plasma and brain pharmacokinetic parameters are displayed in tables 5 and 6.

Table (5) revels that intranasal sumatriptan CS NPs had a $C_{max}$of 405.53±14.21 ng/mL after 60 min. A relatively high sumatriptan absolute bioavailability (78.64%) was achieved after intranasal CS NPs administration. This could be attributed to the penetration enhancing the effect of CS that permitted efficient sumatriptan absorption via nasal epithelium. The brain pharmacokinetic data listed in table 6 showed significantly higher $C_{max}$and $AUC_{0-8}$of sumatriptan following intranasal administration of CS NPs with lower T_{max}indicated the ability of CS NPs to traverse BBB more than the aqueous solution. Furthermore, the high DTE % and DTP% revealed that the IN could target the brain higher than the IV route. The improved brain deposition following intranasal administration of CS NPs could be attributed to the ultimate features of the optimized system. CS is a penetration enhancer that can open the tight junctions by its effect on protein kinase C pathway, occludin and ZO-1 [27]**.**Moreover, NPs with a size less than 100 nm could bypass the BBB via the nasal route [17].

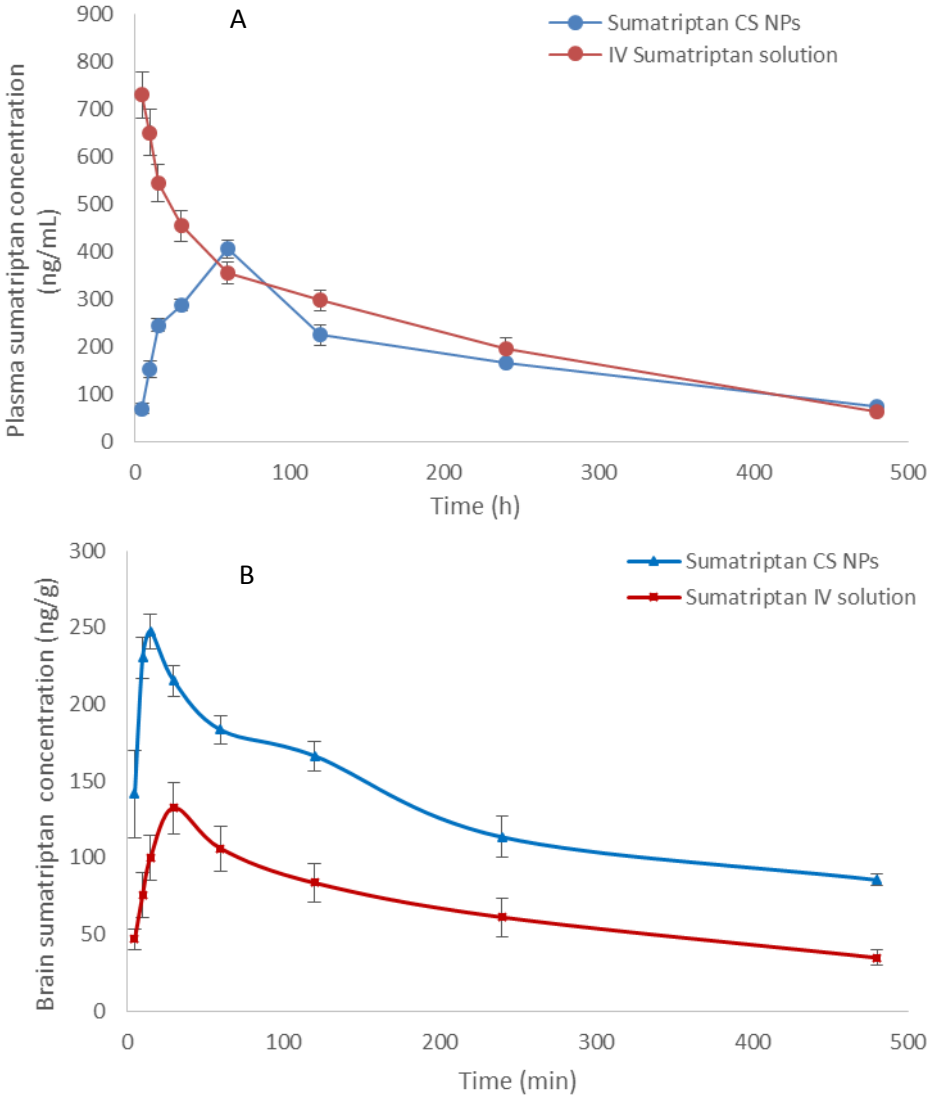

Figure 6: (A) Plasma and (B) brain concentration curves of sumatriptan from nasal chitosan nanoparticles to IV solution. Results are the mean of six replicates at each time interval ±SE.

Table (5): Plasma pharmacokinetic parameters (Mean ± SE, n=6).

Formula	Route of administration	C_{max}(ng/mL)	T_{max}(min)	AUC_{0-8}(ng/mL.h)
Sumatriptan CS NPs	Nasal	405.53±14.210	60	1447.46±29.84
Sumatriptan solution	IV	----	----	1840.22 ±50.11

Table (6): Brain pharmacokinetic parameters (Mean ± SE, n=6).

Formula	Route of administration	C_{max}(ng/g)	T_{max}(min)	AUC_{0-8}(ng/g.h)	DTE %	DTP%
Sumatriptan CS NPs	Nasal	247.37±15.45	15	1027.24±57.61	238.49±5.41	51.12±2.35
Sumatriptan solution	IV	132.31± 9.57	30	639.51±36.74	----	----

IV. Conclusion

From the above results, it could be deduced that BBD was a successful statistical technique to optimize sumatriptan CS NPs with minimum particle size (less than 100 nm) and maximum EE%. CS concentration was found to increase both particle size and EE% while the stirring speed had a negative influence on both size and EE%. Loading sumatriptan into CS NPs could provide an efficient way to control release for 8 h. The optimized CS NPs was able to traverse BBB and accumulate sumatriptan in the brain with a significantly higher extent than IV solutions. These findings may elect nasal CS NPs as a promising candidate for nose-to-brain delivery.

References

[1]. Huang D, Ren L, Qiu C-S, Liu P, Peterson J, Yanagawa Y, Caoa Y-Q. Characterization of a mouse model of headache. *Pain. 157(8), 2016, 1744–1760.*

[2]. Levy D, Jakubowski M, Burstein R, Disruption of communication between peripheral and central trigeminovascular neurons mediates the antimigraine action of 5HT 1B/1D receptor agonists, *Proc. Natl. Acad. Sci. U. S. A. 101, 2004, 4274–4279.*

[3]. Hansraj GP, Singh SK, Kumar P. Sumatriptan succinate loaded chitosan solid lipid nanoparticles for enhanced anti-migraine potential. *Int J BiolMacromol. 81, 2015, 467-76.*

[4]. Chen Y, Liu L. Modern methods for delivery of drugs across the blood-brain barrier. *Adv Drug Deliv Rev. 64(7), 2012, 640-65.*

[5]. Pridgen E. M., Alexis F, Farokhzad O.C. Polymeric nanoparticle drug delivery technologies for oral delivery applications. *Expert Opin Drug Deliv. 12, 2015, 1459-1473.*

[6]. Kalam MA, Khan AA, Alshamsan A. Non-invasive administration of biodegradable nano-carrier vaccines. *Am. J. Transl. Res.9, 2017,15-35.*

[7]. AbdElgadir M, Salim MD, Ferdosh S, Adam A, Khan AJ,Sarker ZI. Impact of chitosan composites and chitosan nanoparticle composites on various drug delivery systems: A review. *Journal of food and drug analysis. 23, 2015, 619-629.*

[8]. Wilson B, SamantaMK, Muthu MS, VinothapooshanG, Design and evaluation of chitosan nanoparticles as novel drug carrier for the delivery of rivastigmine to treat Alzheimer's disease, *Ther. Deliv. 2, 2011, 599–609.*

[9]. Nagpal K., Singh S.K., Mishra D.N., Evaluation of safety and efficacy of brain targeted chitosan nanoparticles of minocycline, *Int. J. Biol. Macromol. 59,2013, 20–28.*

[10]. Agrawal M, Saraf S, Saraf S, Antimisiaris SG, Chougule MB, Shoyele SA, Alexander A. Nose-to-brain drug delivery: An update on clinical challenges and progress towards approval of anti-Alzheimer drugs. *J Control Release. 281, 2018, 139-177.*

[11]. Emami J, Boushehri MS,Varshosaz J. Preparation, characterization and optimization of glipizide controlled release nanoparticles. *Res. Pharm. Sci. 9, 2014, 301-314.*

[12]. Leng D,Thanki K,Fattal E,Foged C, Yang M. Engineering of budesonide-loaded lipid polymer hybrid nanoparticles using a quality-by-design approach. *Int. J. Pharm. 548, 2018, 740-746.*

[13]. CalvoP,Remuñan-Lopez C, Vila-Jato JL, Alonso MJ. Novel hydrophilic chitosan-polyethylene oxide nanoparticles as protein carriers. *J. Appl. Polym. Sci.63, 1997, 125-132.*

[14]. AbulKalam M, Khan AA, Khan S, Almalik A, Alshamsan A. Optimizing indomethacin loaded chitosan nanoparticle size, encapsulation, and release using Box Behnken experimental design. *Int. J. BiolMacromol. 87, 2016, 329-340.*

[15]. Zhang X, Sun M, Zheng A, Cao D, Bi Y, Sun J. Preparation and characterization of insulin loaded bioadhesive PLGA nanoparticles for oral administration. *Eur. J. Pharm. Sci. 45, 2012, 632-638.*

[16]. Elmowafy E, Osman R, El-Shamy AH, Awad GA. Nanocomplexes of an insulinotropic drug: optimization, microparticle formation, and antidiabetic activity in rats. *Int J Nanomedicine. 9, 2014, 4449-65.*

[17]. Abdel-Bar HM, Abdel-Reheem AY, Awad GA, Mortada ND. Evaluation of brain targeting and mucosal integrity of nasally administrated nanostructured carriers of a CNS active drug, clonazepam. *J Pharm Pharm Sci. 16, 2013, 456-69.*

[18]. Huang Y, Lapitsky Y. On the kinetics of chitosan/tripolyphosphate micro and nanogel aggregation and their effects on particle polydispersity. *J. Colloid Interface Sci. 486, 2017, 27-37.*

[19]. Ji J, Wu D, Liu L, Chen J, Xu Y. Preparation, characterization, and in vitro release of folic acid-conjugated chitosan nanoparticles loaded with methotrexate for targeted delivery. *Polym. Bull. 68, 2012, 1707-1720.*

[20]. Ing LY, Zin NM,Sarwar A, Katas H. Antifungal activity of chitosan nanoparticles and correlation with their physical properties. *Int J Biomater. Article ID 632698, 2012.*

[21]. Tsai ML, Bai SW, Chen RH. Cavitation effects versus stretch effects resulted in different size and polydispersity of ionotropic gelation chitosan-sodium tripolyphosphate nanoparticle. *CarbohydrPolym. 71, 2008, 448–457.*

[22]. DizajSM, LotfipourF, Barzegar-JalaliM, ZarrintanMH, AdibkiaK, Box-Behnken experimental design for preparation and optimization of ciprofloxacin hydrochloride-loaded CaCO3 nanoparticles, *J. Drug Deliv. Sci. Technol. 29, 2015, 125–131.*

[23]. Gajra B, Dalwadi C, Patel R. Formulation and optimization of itraconazole polymeric lipid hybrid nanoparticles (Lipomer) using Box Behnken design. *Daru. 23, 2015, 3.*

[24]. Patel BK, Parikh RH,Aboti, P.S.; Development of Oral Sustained Release Rifampicin Loaded Chitosan Nanoparticles by Design of Experiment. *Journal of Drug Delivery. Article ID 370938, 2013.*

[25]. Gryparis EC, Mattheolabakis G, Bikiaris D, Avgoustakis K. Effect of conditions of preparation on the size and encapsulation properties of PLGA-mPEG nanoparticles of cisplatin. *Drug Deliv. 14, 2007, 371-380.*

[26]. Lu B, Lv X, Le Y. Chitosan-Modified PLGA Nanoparticles for Control-Released Drug Delivery. *Polymers (Basel). 11, 2019,pii: E304.*

[27]. Hsu LW, Lee PL, Chen CT, Mi FL,Juang JH, Hwang SM, Ho YC, Sung HW. Elucidating the signaling mechanism of an epithelial tight-junction opening induced by chitosan. *Biomaterials. 33, 2012, 6254-6263.*